AKARI to the depths: The High-z Universe in the Far-IR

David L. Clements[1]

[1]*Astrophysics Group, Physics Department, Blackett Lab., Imperial College, Prince Consort Road, London, SW7 2AZ, UK*

ABSTRACT

The discovery of very high redshift ($z > 4$) highly far-IR luminous ($L > 10^{13} L_{\odot}$) galaxies has proved to be something of a surprise for those who study galaxy formation and evolution in the optical/near-IR. In this review I will discuss what we know about this emerging population, its relationship to more local populations, and what observations with *AKARI*, Herschel and ground based observations have revealed. These include the discovery of a very high redshift far-IR luminous galaxy in the ADF-S, an investigation of the differences between local and high redshift far-IR luminous sources, and the status of searches for far-IR luminous galaxies at $z > 7$. The prospects for further insights into the nature of this population from *AKARI* and other data will also be discussed, as well as the central role that *SPICA* will play in understanding the obscured universe at the highest redshifts.

Keywords: Galaxy evolution

1. INTRODUCTION

The history of energy generation in the universe is the combined history of star formation and supermassive black hole (SMBH) accretion, as well as the formation history of the galaxies that host this activity. Broad constraints can be placed on the history of energy generation by examining the energy content of integrated backgrounds in the universe (Figure 1, and Dole et al. 2006). After the cosmic microwave background (CMB), which is the energy density left behind by the Big Bang, the most energetic cosmic backgrounds are the optical background, peaking at a wavelength of about 1 μm, and the cosmic infrared background (CIB), peaking at a wavelength of about 180 μm. The optical background is made up of the light emitted by stars and AGN across the entire history of the universe that can be directly detected by optical, UV and near-IR instruments. The optical background was thought to include nearly all the energy generated in the universe since the Big Bang until the discovery of the CIB in 1996 (Puget et al. 1996). The CIB originates in the same energy generation processes as the optical background - star formation and SMBH accretion - but the energy of the CIB comes from photons that were absorbed by dust and reprocessed into the rest frame far-IR. The comparable energy densities in the two clearly demonstrates that roughly half of the energy emitted over the history of the universe was absorbed by dust, and cannot be directly traced by observations in the UV/optical/near-IR.

The traditional way of determining the star formation history of the universe is with deep optical observations to detect and measure the redshifted rest-frame UV emission of distant galaxies and AGN, and to use spectral features such as the Lyman-break to determine redshifts (see e.g., Madau & Dickinson 2014 and references therein). Corrections for extinction are then made based on UV spectral slopes or SED fitting, and an overall total luminosity, and thus star-formation rate, can be calculated. The overall picture reached is that the star formation and SMBH accretion rates rise, as we look back in time from $z = 0$, until they reach a peak at $z \sim 2$–3, with a gradual decline to higher redshifts (see the black line in Figure 2). The peak in the star formation rate of the universe at $z \sim 2$–3 has been termed 'cosmic noon'.

However, for dust extinction corrections to the detected rest frame UV flux to work, a galaxy must first be detected in the rest frame UV. The most extreme star forming galaxies in the local universe are the ultraluminous infrared galaxies (ULIRGs, $L_{\rm fir} > 10^{12} L_{\odot}$, see e.g., Sanders & Mirabel 1996 and references therein). These sources are forming stars at rates of >100 $M_{\odot}$/yr, and emit over 95% of their luminosity in the far-IR, from dust at a temperature of ~45 K (Clements et al. 2017). The star forming regions of local ULIRGs are heavily extinguished, with $A_V \gg 20$ mags (Groves et al. 2008; Rangwala et al. 2011). If such sources exist at higher redshift they will be completely absent from the rest frame UV selected samples on which most of our knowledge of the star formation, and accretion, history of the universe is based. Searches for such objects, and the determination of the role of any discovered in the overall history of the universe is thus an essential task if we are not to miss up to half of the energy generation in the universe.

The rest frame far-IR emission of dusty galaxies peaks at a wavelength of ~100 μm. The natural wavelength range in which to search for such sources is thus the far-IR at wavelengths of a 200–1000 μm, corresponding to redshifts of 1 to

Corresponding author: David L. Clements
d.clements@imperial.ac.uk

This document is provided by JAXA.

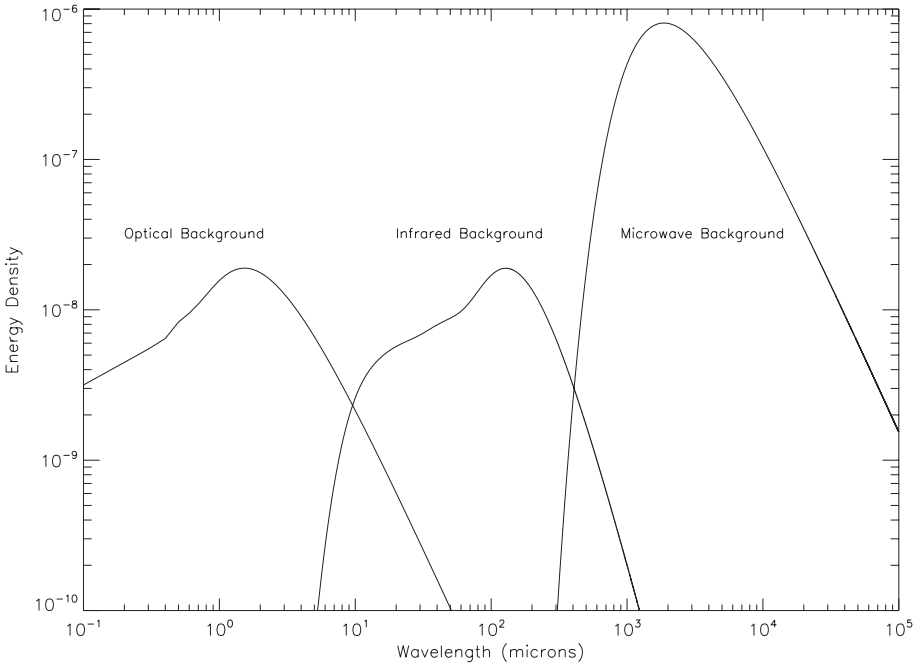

Figure 1. The cosmic optical, infrared and microwave backgrounds. The integrated energy densities of the optical and infrared backgrounds are about the same. From Clements (2014) after an original in Dole et al. (2006).

9 for the peak of the emission. Some work is possible from the ground at the long wavelength end of this range, using instruments such as SCUBA2 at the JCMT, probing the Rayleigh-Jeans tail of the spectral energy distribution (SED) for most redshifts, and benefitting from the well-known negative K-correction (see e.g., Casey et al. 2014), but surveys at these wavelengths are only just beginning to cover the many degree areas necessary to adequately sample a population of rare very high star formation rate (SFR) dusty galaxies. Space-based observations, using satellites working at far-IR wavelengths, such as *AKARI* and *Herschel*, able to cover large areas of the sky, are currently providing our best assessment of the high redshift population of dusty star forming galaxies. Results from such work are beginning to suggest that the history of star formation in the far-IR may be significantly different to that seen in the UV. In particular, analysis of data from the *Herschel* mission in Rowan-Robinson et al. (2016) appears to show that the far-IR derived SFR density remains roughly constant from $z = 3$ to at least $z = 6$ (see Figure 2). While there are large uncertainties in this determination it is interesting to note that a similarly flat SFRD was found by Kistler et al. (2009) in an independent study based on gamma-ray bursts.

The *AKARI* mission plays a strong role in improving our understanding of the high redshift universe in the far-IR. Firstly, through the FIS and IRC surveys it improves out knowledge of ULIRGs and related objects in the local universe, setting the local baseline against which more distant objects can be compared. The most valuable role in the long term, though, is likely to be the establishment of deep survey fields that will be studied by many future generations of telescope. In the rest of this paper I will examine each of these different aspects of *AKARI*'s contribution in turn. In the next section I will discuss the establishment of the low redshift baseline. After that I will discuss the deep survey fields in the NEP and ADF-S as well as highlighting some recent results. Finally I will look forward to *SPICA* and its potential for much deeper large area surveys.

2. THE LOW REDSHIFT BASELINE

Much of our knowledge of ULIRGs in the local universe is based on data from the *IRAS* satellite, which surveyed almost the entire sky at four mid-to-far-IR wavelengths (12, 25, 60 and 100 μm) for 10 months after its launch in 1984. The point source catalogs derived from this data are essentially all based on flux limited selection at 60 μm, so all of our local ULIRGs are 60 μm selected objects. More recent surveys, whether with ground-based submm instruments or with *Herschel*, are based on selection at longer wavelengths, largely 850 μm from the ground or 250 μm for *Herschel*. The dust SED of galaxies peaks at a rest frame wavelength of typically 100 μm, which means that our sources are selected in two contrasting ways - at wavelengths shorter than the peak in the local universe, and at wavelengths longer than the peak in the high redshift universe (except for *Herschel* sources at $z > 1.5$ where the SED peak is shifted longward of the 250 μm band; more of this later). There is thus the possibility that these different selection approaches might lead to the selection of galaxies with subtly different properties, such as dust temperature. There is in fact some indication that this is the case (Clements et al. 2017), with *IRAS* selected ULIRGs appearing to have higher dust temperatures (and thus higher 60 μm fluxes) than higher redshift, *Herschel* selected counterparts.

This document is provided by JAXA.

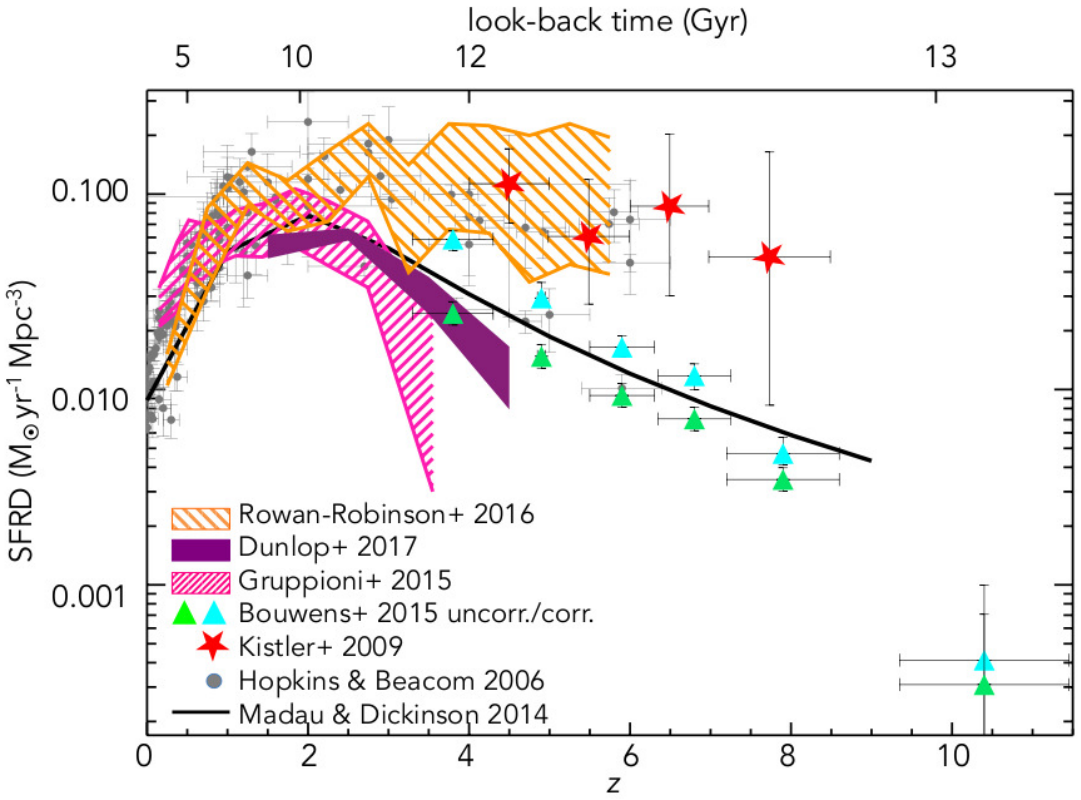

Figure 2. The redshift evolution of the star formation rate density (figure from Gruppioni et al. 2017) including an optical/UV compilation by Hopkins & Beacom (2006), the IR SFRD from Gruppioni et al. (2015), the Rowan-Robinson et al. (2016) *Herschel* analysis, the SFRD evolution derived from ALMA data (Dunlop et al. 2017), the best-fit model by Madau & Dickinson (2014) to dust-corrected UV and IR data, dust-corrected and uncorrected UV data from Bouwens et al. (2015) and the high-z GRB determination from Kistler et al. (2009).

The most sensitive band in the *AKARI* all sky FIS survey (Yamamura et al. 2017), unlike *IRAS*, is the 90 μm. The FIS catalogue, therefore, is essentially 90 μm selected, providing a complementary longer wavelength selection closer to the SED peak than for *IRAS*. Kilerci Eser et al. (2014) were the first group to use the FIS all sky survey to produce a catalog of ULIRGs through matching *AKARI* sources to optical sources with known redshifts from the SDSS or 2DF-GRS surveys. This followed initial cross matching of *AKARI* all sky survey sources to SDSS objects by Goto et al. (2011). Kilerci Eser et al. (2014) identified 118 ULIRGs and one HLIRG ($L_{\rm fir} > 10^{13} L_\odot$) in their analysis, of which 40 ULIRGs and the HLIRG do not appear in previous catalogs. The redshift range for the new ULIRGs goes from $z = 0.05$ to $z = 0.487$. Comparison of the properties of these 90 μm selected ULIRGs with those of the *IRAS* 60 μm selected ULIRGs will be the first step in seeing if there are biases in ULIRG selections at different wavelengths. Version 2 of the FIS catalog, with improved photometry, will be very useful for this task.

The IRC all sky survey (Ishihara et al. 2010) also has a role to play in setting the low redshift baseline for DSFGs, and guiding future observations of their high redshift equivalents. This survey, at 9 and 18 μm, fills gaps in the spectral coverage of other surveys. In combination with other data from e.g., *WISE, IRAS* and *ISO*, we now have good coverage of the mid-IR SEDs of a large number of objects in the nearby universe, including many local ULIRGs. Murata et al. (2017), is a good example of this kind of analysis applied to local ULIRGs and other star forming galaxies. They find that merger systems, such as ULIRGs, have less significant polycyclic aromatic hydrocarbon (PAH) emission compared to the emission from large dust grains than non-merger galaxies. This effect is ascribed to the destruction of PAHs by a combination of a stronger radiation field in these systems and to shocks produced during the mergers.

The combination of IRC and other data provides good coverage of SEDs from the optical through to wavelengths of ~24 μm. There is then a gap in available survey data up to the *IRAS* 60 μm band. This wavelength range is potentially important, especially for high redshift studies (see e.g., Gruppioni et al. 2017), but we will have to await the launch of *SPICA* for this missing band to be filled.

3. THE *AKARI* DEEP FIELDS

3.1. Observations of the *AKARI* Deep Fields

With only a 68.5 cm telescope, *AKARI* was unable to scan the whole sky to depths sufficient to detect significant numbers of sources at high redshifts ($z \gg 0.5$). However, significantly deeper observations were obtained with both the FIS and

This document is provided by JAXA.

Name	RA	Dec	Size
AKARI NEP Wide Field	18:00:00	+66:30:00	5.8 deg^2
AKARI NEP Deep Field	18:56:00	+66:30:00	0.5 deg^2
AKARI Deep Field South	04:44:00	-53:20:00	12 deg^2

Table 1. Basic parameters of the *AKARI* deep fields. Note that the NEP field has both wide and deep components.

IRC in two deep fields, basic details of which are given in Table 1. These fields are at high ecliptic latitudes and lie in the continuous viewing zone for most astronomical missions. High ecliptic latitude regions will also be those most frequently observed by scanned survey missions which, in the past, have included both *IRAS* and *Planck*. They are thus among some of the best studied fields on the sky.

The *AKARI* NEP field was observed with the IRC at nine different near- to mid-IR wavelengths, 2.4 μm, 3.2 μm, 4.1 μm, 7.0 μm, 9.0 μm, 11.0 μm, 15.0 μm, 18.0 μm, and 24.0 μm, providing nearly continuous coverage across this band. The survey was conducted in two different 'wedding cake' layers, a shallow survey over 5.8 deg^2 and a deep survey over 0.5 deg^2 with 5σ sensitivities in the tens of μJy level in most bands (see Murata et al. 2014 for details). A wide range of complementary data has since been obtained in the NEP region, including *Chandra* X-ray observations, *GALEX* UV, ground-based optical and near-IR (see e.g., Burgarella et al. 2017), *Herschel* from the PACS and SPIRE instruments, SCUBA2 submm, and 20 cm radio observations (White et al. 2010). Most of these observations have so far concentrated on the deep survey region, but the larger area survey is gradually being covered. A diagram of the observations in the NEP survey fields is shown in Figure 3.

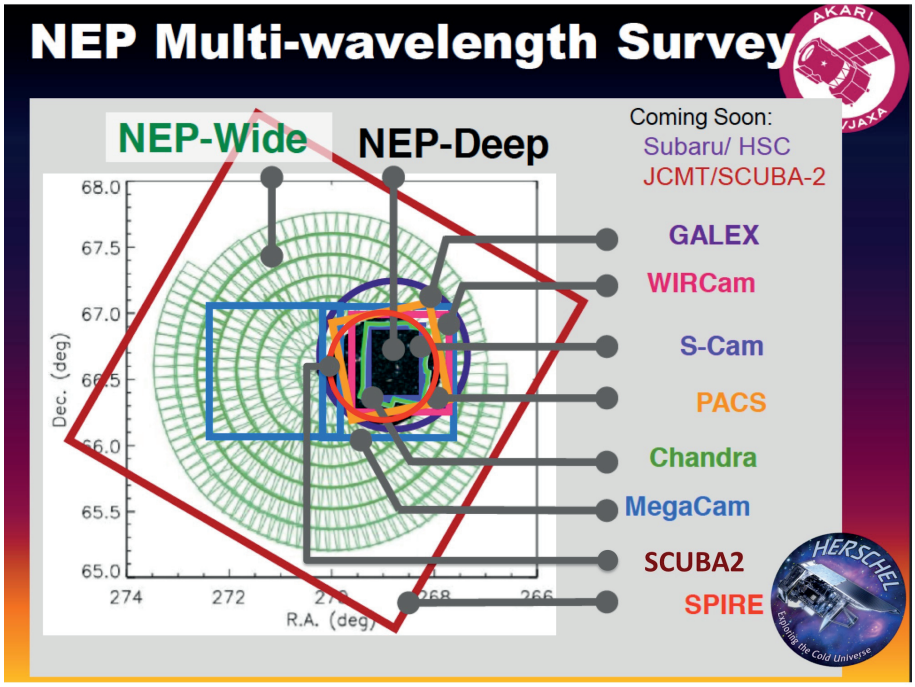

Figure 3. The NEP survey fields and additional data available or being observed in the near future. Courtesy of D. Burgarella.

The *AKARI* deep field south (ADF-S) covers a ~12 deg^2 rectangular region of very low foreground cirrus emission close to the south ecliptic pole (Shirahata et al. 2009). The entire area was covered by deep observations with the FIS at 65, 90, 140 and 160 μm, reaching a 90 μm 60% completeness limit of 28 mJy (Sedgwick et al. 2011). IRC imaging at a number of different mid-IR wavelengths was obtained over 0.8 deg^2 within this field. Data at a wide ranger of other wavelengths is available for all or part of the ADF-S. This includes *Spitzer* observations at 24 and 70 μm (Clements et al. 2011) and *Herschel* 250, 350 and 500 μm observations over the entire field (Oliver et al. 2012), 1.25 mm imaging over 0.25 deg^2 (which have since been followed up with ALMA), and 20 cm radio observations over 2.5 deg^2 (White et al. 2012). Diagrams of the observations in the ADF-S can be found in Clements et al. (2017).

It should be noted that this list of observations in place and underway for these fields is likely to be incomplete, and additional followup studies are being added all the time.

This document is provided by JAXA.

3.2. From Counts to Luminosity Functions

The most basic results than can come from surveys such as the *AKARI* deep fields are number counts plots. These can be found for the NEP in Pearson et al. (2010, 15 μm counts), Pearson et al. (2014, 18 μm counts) and Murata et al. (2014, 2.2 to 11 μm counts) as well as in the current volume. The results from these counts observations are consistent with existing data from *ISO* and *Spitzer* and confirm the existence of a strong evolutionary bump in the counts at fluxes of about 0.2–0.4 mJy in the longer wavelength bands (see Pearson et al., in this volume). Comparison to models suggests that this bump in the counts is due to a strongly evolving population of luminous starbursts at redshifts greater than 1.

While counts are an excellent first step in any analysis, a full understanding of the evolving population only comes when redshifts can be obtained and the evolution of the luminosity function with redshift can be determined. The combination of optical and near-IR images of the NEP deep field, from the CFHT with the 9 band near-to-mid-IR coverage from *AKARI* allows for both accurate photo-z estimation and determination of 8 and 12 μm rest-frame fluxes out to $z > 1$ without the extrapolations necessary in some other work (Goto et al. 2015). The resulting evolving luminosity functions demonstrate the rapid evolution of luminous infrared galaxies from $z = 0$ to $z \sim 1.5$, and especially the rapid rise in the contribution of the most luminous sources, ULIRGs, to the star formation rate and far-IR density and the total infrared luminosity (see Figure 4, from Goto et al. 2015).

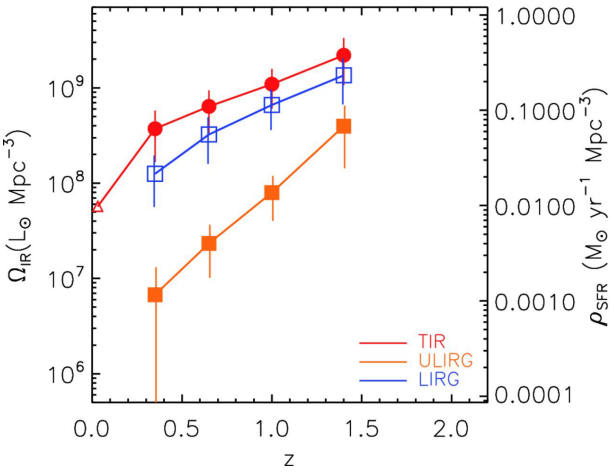

Figure 4. The redshift evolution of total infrared luminosity from all classes of galaxy, which is also a measure of star formation rate, and the contributions to this from luminous and ulitraluminous infrared galaxies derived form NEP Deep survey data. Note the steep rise in the contribution from ULIRGs over the redshift range probed by these observations. From Goto et al. (2015).

3.3. The High Redshift Universe

AKARI observations themselves are not deep enough to provide significant samples of galaxies at $z \gg 1.5$, but by defining the NEP and ADF-S fields *AKARI* has prepared the ground for other observations to push to higher redshift. In the search for high redshift DSFGs the data sets that are most important at the moment are those from *Herschel*, especially when combined with data at longer submm wavelengths. However, as we shall see, data at longer wavelengths will play a major role in the future, for example from the SPT or NIKA2 instruments.

Even with the strong evolution seen in the population in studies such as Goto et al. (2015), high redshift DSFGs are still rare on the sky. Large areas of the sky must thus be searched to find candidates for further investigation. The *Herschel* surveys HerMES (covering a total of ~380 deg^2; Oliver et al. 2012) and H-ATLAS (covering an area of about 630 deg^2; Eales et al. 2010) are the main resources for this work. Candidate very high redshift DSFGs can be selected on the basis of their colour in the 250, 350 and 500 μm bands observed by the SPIRE instrument. Since the far-IR emission of a DSFG peaks at a wavelength of ~100 μm, the colour of such an object in these bands gets redder with increasing redshift. Out to redshifts ~2 the observed SED will peak in the 250 μm band, from redshifts of 2 to 4 it will peak in the 350 μm band, and at redshifts > 4 it will peak in the 500 μm band. Candidate high redshift DSFGs can thus be sought by looking for sources with $F500 > F350 > F250$.

These searches have been highly successful. They have uncovered specific extreme sources that can be studied in detail, such as the $z = 6.34$ source HFLS3 (Riechers et al. 2013) which, until very recently, was the highest redshift DSFG known. They have also uncovered a significant population of these '500-riser' galaxies (Dowell et al. 2014; Asboth et al. 2016) whose number counts, at ~2 /deg^2, are substantially in excess of almost all current models. These two HerMES-based studies have found over 500 of these 500-riser sources, while work with similar selection techniques is underway in the larger H-ATLAS survey (Oteo et al., in prep). Spectroscopic redshift confirmation for a sample of sources this large is not easy. Determination the correct optical cross-identification for a given SPIRE source is hard because of the 36 arcsec beam of *Herschel* at 500 μm. Continuum imaging at arcsecond resolution using mm/submm interferometers, such as NOEMA,

This document is provided by JAXA.

ALMA or the SMA (e.g., Greenslade et al., in prep), is usually necessary to establish an optical/NIR identification. When available such cross-IDs are usually too faint for optical/NIR spectroscopy because of the combination of redshift and dust obscuration. Most progress in redshift determination for this population has been a result of mm/submm spectroscopy, looking for the redshifted CO and [C II] lines. However, this progress has been slow since the necessary integration times for broad spectral range instruments, such as SWARM on the SMA or EMIR on the IRAM 30 m, are long, or because the current observing efficiency of spectral scan mode at ALMA is low. Nevertheless, redshifts are now available for up to 20 individual 500-riser sources, almost all of which are above a redshift of 4, confirming the efficacy of the selection method (see e.g., Asboth et al. 2016).

The luminosities of these sources have to be $>\sim 10^{13} L_{\odot}$/yr for them to be detectable by SPIRE at these high redshifts. This means that they are either extreme sources, forming stars at rates >1000 $M_{\odot}$/yr, that they might be blends of several individual sources within the SPIRE beam, or that they have their observed fluxes boosted by strong gravitational lensing. We already know that the brightest 500 μm sources in SPIRE surveys include a large fraction of strongly lensed sources (e.g., Wardlow et al. 2013). ALMA observations of a sample of 29 SPIRE sources at more moderate fluxes (Bussmann et al. 2015) finds that only six are the result of strong lensing, but that up to 70% appear to be multiple, though with some indication that these multiple sources may be physically associated, possibly as separate components of objects being formed from galaxy interactions or mergers.

The highest redshift DSFG with spectroscopic confirmation currently known is SPT0311-58, a 500-riser associated with a 1.4 mm source discovered in the South Pole Telescope (SPT) SZ survey and with a measured redshift of 6.900±0.002 (Strandet et al. 2017).

3.4. **Pushing to the Highest Redshifts**

The success of using SPIRE colours to identify a population of $z > 4$ DSFGs leads to the obvious question of whether this type of approach can be pushed to still higher redshifts. Such a study would require a survey or followup observations at wavelengths longer than 500 μm. Fortunately such data is available in some of the *Herschel* survey regions thanks to the SCUBA2 legacy surveys (e.g., Geach et al. 2017), the AzTEC/ASTE observations in ADF-S (Hatsukade et al. 2011), or pointed followup of specific objects. Spectroscopic followup of objects selected from such data sets has at least the same difficulties as those that apply to the 500-riser sources, if not worse. The first such '870-riser' - a source whose flux rises between 500 and 870 μm, as determined by observations with APEX/LABOCA - to be properly characterised is ADFS-27 (Riechers et al. 2017). This object, found in the HerMES SPIRE observations of ADF-S, has a spectroscopic redshift of $z = 5.655$ and is made up of a pair of galaxies at the same redshift. Their interaction or ongoing merger is thought to have triggered the massive starburst (SFR $\sim$ 2400 $M_{\odot}$/yr) powering this very luminous source (see Figure 5).

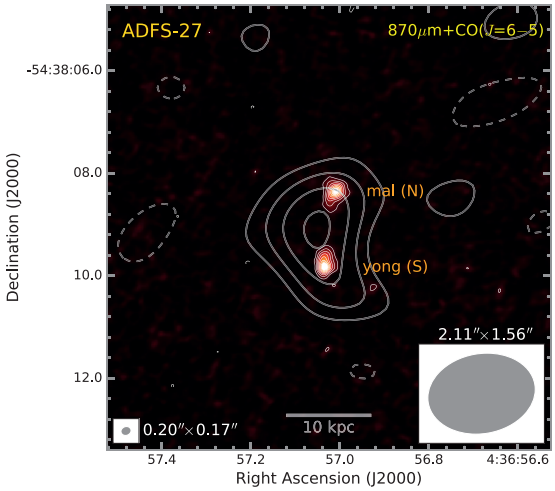

Figure 5. Continuum image of the $z = 5.655$ source ADFS-27 obtained with ALMA at 870 μm overlaid on contours showing CO (6–5) line emission obtained at lower angular resolution (beam sizes shown at bottom left and right). The two continuum sources lie at the same redshift and are likely to be merging galaxies 10 kpc apart. From Riechers et al. (2017).

DSFGs at still higher redshift are likely to be even more elusive since they will be too faint to be detected by SPIRE in any of its three bands. However, while they will be undetectable by SPIRE, such sources would still be detectable from the ground at wavelengths around 1mm, and would thus appear as 'SPIRE-dropouts' - seen in mm/submm data but absent from matching *Herschel* images. A number of such sources have been identified in the ADF-S, by comparing the 1.1 mm data of Hatsukade et al. (2011) with SPIRE data, as well as in a number of other fields (Greenslade et al., in prep). So far,

This document is provided by JAXA.

despite significant observational effort, we have yet to secure a spectroscopic redshift for a SPIRE-dropout. SED analysis, however, suggests that the candidate objects so far identified lie at $z \sim 7$.

4. CONCLUSIONS: FROM *AKARI* TO ALMA AND *SPICA*

AKARI has contributed to the understanding of DSFGs in a number of ways - through improving our understanding of their local equivalents, through counts and luminosity function analysis in the deep fields, and through establishing the NEP and ADF-S deep fields as key deep survey fields for the future. *AKARI* also adds complementary data to the study of sources selected at longer far-IR wavelengths by *Herschel*. The immediate future for this field lies in the continued analysis of sources selected from *Herschel* surveys and from the developing array of surveys by instruments such as SCUBA2, NIKA2 and the SPT at longer mm/submm wavelengths at 850 μm to 2 mm. Followup of these sources, and especially mm/submm spectroscopy for redshift determination, will be undertaken by the current generation of mm/submm interferometers, including ALMA, NOEMA and the SMA, as well as sensitive single dish instruments such as the IRAM 30 m or the LMT. Key to these redshift determinations will be the ability to study a wide range of frequencies either through spectral scannning at ALMA, or with large instantaneous bandwidth instrumentation such as SWARM at the SMA or the RSR. Detailed study of individual objects, once their nature is confirmed, will be undertaken by the JWST. However, at the high, $z > 6$, redshifts likely to be of most interest, JWST will be limited to observing the rest frame uv to near-IR. Longer wavelengths are key to understanding such heavily dust obscured systems. Ground based interferometers such as ALMA have the wavelength coverage and sensitivity to study some of the most interesting transitions at these redshifts (e.g., the [C II] line at 157 μm), but many studies, such as the development of PAHs, require observations in the rest frame mid-IR, which will be redshifted to the far-IR for these objects. Future space-based far-IR observatories, such as *SPICA* (e.g., Gruppioni et al. 2017; Spinoglio et al. 2017) will thus be key to a full understanding of this emerging population and the determination of its place in the history of galaxy formation and evolution.

ACKNOWLEDGMENTS

It is a pleasure to thank the SOC of the 4th AKARI conference for inviting me to present this review, and Kohno-san for hosting me at Tokyo University. I would also like to thank my PhD students Josh Greenslade and Tai-An Cheng for useful discussions on this paper.

REFERENCES

Asboth V., et al., 2016, MNRAS, 462, 1989
Bouwens R. J., et al., 2015, ApJ, 803, 34
Burgarella, D., et al., 2017, this volume
Bussmann R. S., et al., 2015, ApJ, 812, 43
Casey C. M., Narayanan D., Cooray A., 2014, PhR, 541, 45
Clements, D.L., Pearson, C., Farrah, D., et al., 2017, MNRAS, submitted
Clements, D.L., 2014, *Infrared Astronomy: Seeing the Heat*, published by CRC press
Clements D. L., Bendo G., Pearson C., et al., 2011, MNRAS, 411, 373
Dole H., Lagache, G., Puget, J-L., et al., 2006, A&A, 451, 417
Dowell C. D., et al., 2014, ApJ, 780, 75
Dunlop J. S., et al., 2017, MNRAS, 466, 861
Eales S., et al., 2010, PASP, 122, 499
Geach J. E., et al., 2017, MNRAS, 465, 1789
Goto T., et al., 2015, MNRAS, 452, 1684
Goto, T., Arnouts, S., Malkan, M., et al., 2011, MNRAS 414, 1903
Groves B., Dopita M. A., Sutherland R. S., et al., 2008, ApJS, 176, 438
Gruppioni C., et al., 2017, PASA, in press, arXiv:1710.02353
Gruppioni C., et al., 2015, MNRAS, 451, 3419
Hatsukade B., et al., 2011, MNRAS, 411, 102
Hopkins A. M., Beacom J. F., 2006, ApJ, 651, 142
Ishihara D., et al., 2010, A&A, 514, A1
Kilerci Eser E., Goto T., Doi Y., 2014, ApJ, 797, 54
Kistler M. D., Yüksel H., Beacom J. F., Hopkins A. M., Wyithe J. S. B., 2009, ApJ, 705, L104
Madau P., Dickinson M., 2014, ARA&A, 52, 415
Murata K. L., Yamada R., Oyabu S., et al., 2017, MNRAS, 472, 39
Murata K., Pearson C. P., Goto T., Kim S. J., Matsuhara H., Wada T., 2014, MNRAS, 444, 2346
Oliver S. J., et al., 2012, MNRAS, 424, 1614
Pearson C. P., et al., 2014, MNRAS, 444, 846
Pearson C. P., et al., 2010, A&A, 514, A8
Puget J.-L., Abergel A., Bernard J.-P., et al. 1996, A&A, 308, L5

This document is provided by JAXA.

Rangwala N., Maloney, Philip R., Glenn, Jason, et al., 2011, ApJ, 743, 94
Riechers D. A., et al., 2017, ApJ., in press
Riechers D. A., et al., 2013, Natur, 496, 329
Rowan-Robinson M., et al., 2016, MNRAS, 461, 1100
Sanders D. B., Mirabel I. F., 1996, ARA&A, 34, 749
Sedgwick C., et al., 2011, MNRAS, 416, 1862
Shirahata M., et al., 2009, ASPC, 418, 301
Spinoglio L., et al., 2017, PASA in press, arXiv:1710.02189
Strandet M. L., et al., 2017, ApJ, 842, L15
Wardlow J. L., et al., 2013, ApJ, 762, 59
White G. J., et al., 2012, MNRAS, 427, 1830
White G. J., et al., 2010, A&A, 517, A54
Yamamura, I., et al., 2017, this volume

This document is provided by JAXA.